Research Square

Preprints are preliminary reports that have not undergone peer review.
They should not be considered conclusive, used to inform clinical practice,
or referenced by the media as validated information.

Rising tidal low waters disproportionately increase drainage constraints in low-elevation coastal zones

Henning Müller

henning.mueller@tu-braunschweig.de

Technische Universität Braunschweig

Christan Jordan

Leibniz University Hannover

Julius Thierfeldt

Technische Universität Braunschweig

Julius Engelmann

Technische Universität Braunschweig

Gabriel David

University of Rostock

Nils Goseberg

Technische Universität Braunschweig

Kai Schröter

Technische Universität Braunschweig

Article

Keywords:

Posted Date: November 24th, 2026

DOI: https://doi.org/10.21203/rs.3.rs-11762082/v1

License: This work is licensed under a Creative Commons Attribution 4.0 International License.
Read Full License

Additional Declarations: No competing interests reported.

Rising tidal low waters disproportionately increase drainage constraints in low-elevation coastal zones

Henning Müller[1*], Christian Jordan[2], Julius Thierfeldt[1], Julius Engelmann[1], Gabriel David[3], Nils Goseberg[4,5], Kai Schröter[1]

[1]Leichtweiß Institute for Hydraulic Engineering and Water Resources, Division of Hydrology and River Basin Management, Technische Universität Braunschweig, Braunschweig, 38106, Germany.
[2]Ludwig-Franzius-Institute for Hydraulic, Estuarine and Coastal Engineering, Leibniz Universität Hannover, Hannover, 30167, Germany.
[3]Coastal Engineering; Faculty for Agriculture, Civil and Environmental Engineering, University of Rostock, Rostock, 18059, Germany.
[4]Leichtweiß Institute for Hydraulic Engineering and Water Resources, Division of Hydromechanics, Coastal and Ocean Engineering, Technische Universität Braunschweig, Braunschweig, 38106, Germany.
[5]Coastal Research Center, Joint Central Institution of Leibniz Universität Hannover and Technische Universität Braunschweig, Hannover, 30419, Germany.

*Corresponding author(s). E-mail(s): henning.mueller@tu-braunschweig.de;

Abstract

Coastal lowlands are dynamic, densely populated environments where water and flood management is often shaped by controlled drainage to the sea. Gravity-driven drainage is only possible when coastal water levels fall below inland water levels. When coastal water levels remain elevated, drainage is constrained and inland flood hazard increases. However, how long and how often such periods occur has not been systematically quantified. Here, we frame periods of constrained drainage as events and quantify their duration, frequency and sensitivity to changing water levels. For this, we link tidal observations with inland reference levels at 79 outlets along the German North Sea coast and its estuaries. At all

sites, constraint durations increase non-linearly with rising tidal low water levels, while neighbouring sites can respond differently to the same change. Across sites, a median rise in mean low water of 0.32 m turns a 20-year constraint event into a 2-year event. Such shifts, whether driven by sea-level rise, altered surge and tidal dynamics, or land subsidence, challenge flood management and require anticipatory adaptation beyond measures for extreme sea levels.

Keywords: coastal drainage, water management, low-elevation coastal zones, tide

Introduction

Low-elevation coastal zones (LECZs), defined here as areas below 10 m elevation, are home to hundreds of millions of people worldwide [1] and generate about 14 % of the world's gross domestic product, while facing significant risks from climate change that threaten both societal stability and economic functions [2]. Climate change-related sea-level rise (SLR) and more frequent weather extremes are increasing flood hazards in LECZs [3–6], driving adaptation needs. In many low-lying, tidally influenced coastal regions, dikes protect the hinterland from storm surges and seaward flooding. However, by restricting natural drainage to the sea, they also require drainage networks with tidal gates (one-way outlets) and pumping stations to manage pluvial and fluvial inflows and prevent landside flooding of LECZs. Such systems are widely operated in Europe [7–9], Asia [10, 11], North America [12, 13], and Australia [14]. Operating such systems involves actively regulating water levels and continuously balancing competing objectives: safeguarding communities, economic assets, and critical infrastructure from inundation, while preserving suitable conditions for economic activities, predominantly agriculture, and ecosystems. Effective drainage management critically depends on the available drainage capacity, defined here as the hydraulic and technical ability of a drainage system to store and discharge water. In diked LECZs, drainage capacity depends on the hydraulic gradient between inland water levels and the downstream marine or estuarine system. This gradient determines whether water can be discharged by gravity through tidal gates (hereafter, free drainage). When downstream water levels exceed inland water levels, free drainage is not possible and pumping is required to prevent inland flooding. Along the German North Sea coast, around 80 % of coastal drainage systems rely at least partly on free drainage through tidal gates, whereas the remaining 20 % depend entirely on pumping [15].

In tidal environments, tidal dynamics, superimposed by storm surges and long-term sea level variability, are a key factor in reduced drainage capacity [14, 16, 17]. While pumping stations can discharge water throughout the full tidal cycle (within their technical limits), tidal gates primarily prevent inundation during high tides and facilitate free drainage of the hinterland during low-tide conditions [7, 14, 18]. As a result, free drainage is inherently intermittent, and drainage capacity is not a fixed property of the infrastructure alone but a time-varying function that reflects the interaction between the drainage system and the dynamics of seaside water levels. When coastal water levels remain high even at low tide, water can no longer drain freely from

the hinterland to the sea (Figure 1a). Water accumulating inland must then be temporarily stored or pumped out to prevent inland water levels from exceeding critical thresholds.

Previous studies have recognized the reduced drainage capacity of LECZs under elevated low-tide levels [14, 19]. The concept of a drainage window (DW), a period of potential free drainage, has been used to quantify and compare free drainage of estuarine catchments under SLR conditions, linking elevated low tides to an increased flood hazard in diked LECZs [14, 20].

Flood hazard and risk assessments in LECZs increasingly recognize that coastal flooding often results from compound events, in which several drivers occur together or in close succession [21]. Previous studies have therefore examined extreme coastal water levels and tides in combination with river flooding [6, 22], precipitation [5, 7, 23–25], and large-scale weather patterns [26]. Together, these studies indicate that flooding in deltas and estuaries can arise from interacting drivers, and their combination can lead to high impacts even if the impacts of either driver individually would not be particularly severe. For example, Bormann et al. [7] have shown that the co-occurrence of heavy, but not extreme, rainfall with moderately elevated coastal water levels can already result in elevated inland water levels due to the reduction of drainage capacity in a German LECZ catchment.

In diked LECZs, flood hazard therefore depends not only on conditions on either side of the dike, but also on how coastal and inland water levels interact through the drainage system. This interaction is particularly important where inland water is discharged by free drainage, which can only lower inland water to the operational target level when tidal low waters (TLWs) fall below this level. We refer to periods in which successive TLWs remain above the operational target level as drainage constraints. During drainage constraints, drainage capacity is limited to inland storage and pumping, and coastal water level dynamics directly determine when, and for how long, these periods occur. Drainage constraints are particularly relevant because they can increase flood hazard in the hinterland, especially when they coincide with rainfall or other flood-generating processes [24, 27].

Existing drainage-specific indicators, such as DWs, quantify potential periods of free drainage during TLW phases [14]. This process understanding, however, has not been carried into statistical compound flood analyses, which typically represent coastal forcing through mean or maximum sea levels aggregated in time or space [5–7, 22–26, 28]. These metrics do not capture TLWs and cannot resolve the intermittent nature of free drainage, nor whether, or for how long, elevated coastal water levels constrain it. To our knowledge, drainage constraints have not been characterized as events with statistical properties, such as how often they occur, how long they persist, and how these properties vary over time and between regions.

As a result, an important link between coastal water level dynamics and the operational state of inland drainage systems remains insufficiently represented in flood hazard assessments for LECZs. Addressing this gap would better align flood hazard assessment with the operational requirements of drainage management and support the adaptation of drainage infrastructure to changing coastal and hinterland conditions.

To address this gap, we answer the following questions: 1) How do coastal and inland water levels jointly determine drainage constraints? 2) How do these constraints and their sensitivity to changes in coastal and inland water levels vary across drainage outlets? 3) How much change in these water levels is required for prolonged drainage constraints to become substantially more frequent?

For this, we analyse 79 coastal drainage outlets along the German North Sea coast, which control the drainage of LECZs either directly into the North Sea or into its tidally influenced estuaries (Figure 1b). At each outlet, we combine 37 years of spatially interpolated TLWs with airborne laser scanning (ALS)-derived inland reference levels, which approximate operational target levels, to statistically analyse the duration and frequency of periods during which TLWs remain above the corresponding inland reference level. By focusing explicitly on these periods of constrained drainage, we quantify their duration and frequency consistently across sites, enabling comparison among outlets under present-day conditions. We further assess how sensitive these constraints are to changes in the difference between mean low water (MLW) and the inland reference level (hereafter, relative water level), for example due to SLR or land subsidence. We show that 1) constraint duration responds non-linearly to the relative difference between MLW and inland reference levels, 2) the sensitivity of individual drainage systems to identical relative water level changes varies strongly and is governed primarily by local rather than regional conditions and 3) relative water level changes of a few decimetres can markedly increase the frequency of prolonged drainage constraints, with projected SLR sufficient to make such constraints substantially more frequent over the coming decades.

Results

LECZ drainage constraints increase non-linearly with rising TLW levels

Free drainage at a coastal outlet is only possible when the water level on the seaward side is lower than the inland water level. However, free drainage only reduces flood hazard effectively if coastal water levels fall low enough for the inland water to drain below a prescribed reference level (z). When successive TLWs remain above this threshold, free drainage is insufficient, and a drainage constraint spell develops (Figure 2a). Lower coastal water levels provide more frequent DWs, whereas coastal water levels that are elevated relative to the inland reference level result in longer constraint spells without sufficient free drainage. We use the 2-year return level ($RL2$) of constraint spell duration to characterize recurrent but substantial drainage constraints.

Across the 79 drainage outlets analysed along the German North Sea coast, the 2-year constraint spell duration increases non-linearly with rising MLW relative to the inland reference level (Figure 2b). All outlet-specific constraint curves exhibit the same general form: constraint durations remain short when MLW lies several metres below z, but increase rapidly as the MLW approaches and exceeds z. Over only a few decimetres of rising MLW, the 2-year constraint duration can increase by more than an order of magnitude. This response arises because increasing MLW causes

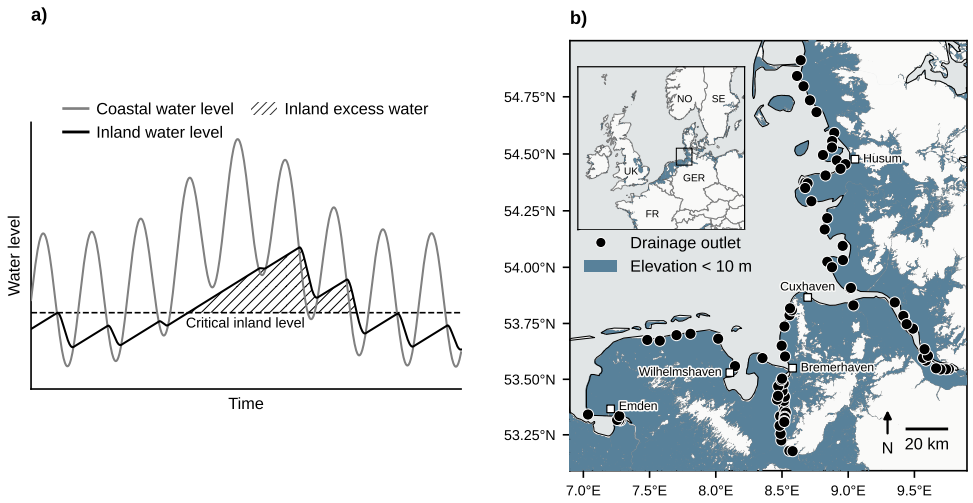


Fig. 1 Drainage constraints in low-elevation coastal zones (LECZs) along the German North Sea coast. a) Conceptual illustration of the interaction between coastal and inland water levels. Free drainage is constrained when coastal water levels remain too high relative to inland levels, which can lead to the accumulation of excess inland water above a critical inland level; **b)** Location of the 79 coastal drainage outlets included in the analysis (black circles). Blue shading indicates LECZs below 10 m elevation (GLO-30 DEM [29]). The inset shows the location of the study region within northwestern Europe with LECZs in blue (Global LiDAR Lowland DTM [30]).

previously separated constraint spells to merge into longer spells, until nearly all TLWs exceed the reference level and free drainage is continuously constrained. The drainage constraint curves therefore show how strongly drainage constraints are controlled by coastal water levels. Because each curve represents the $RL2$, every point corresponds to the constraint duration associated with the same annual exceedance probability. Rising MLW shifts this return level towards longer durations, meaning that longer constraint spells occur with the same frequency.

At their present-day operating levels, most drainage systems currently cluster in the range between 0 and 30 consecutive TLWs (up to about 15 days), with progressively fewer systems at longer constraint durations (Figure 2c). This variability highlights that prolonged drainage constraints are already a present-day operational condition rather than a future challenge in many coastal catchments.

Local sensitivity to relative water level rise varies strongly among drainage systems

As the drainage constraint curves are non-linear, an identical increase in relative water level can lead to markedly different changes in constraint duration, depending on where the operating point of an outlet lies on its constraint curve. We quantify this present-day sensitivity using the local constraint curve slope $\Delta RL2/\Delta x$ (S_{local}), defined as the increase in the 2-year constraint duration associated with a 0.1 m increase in relative

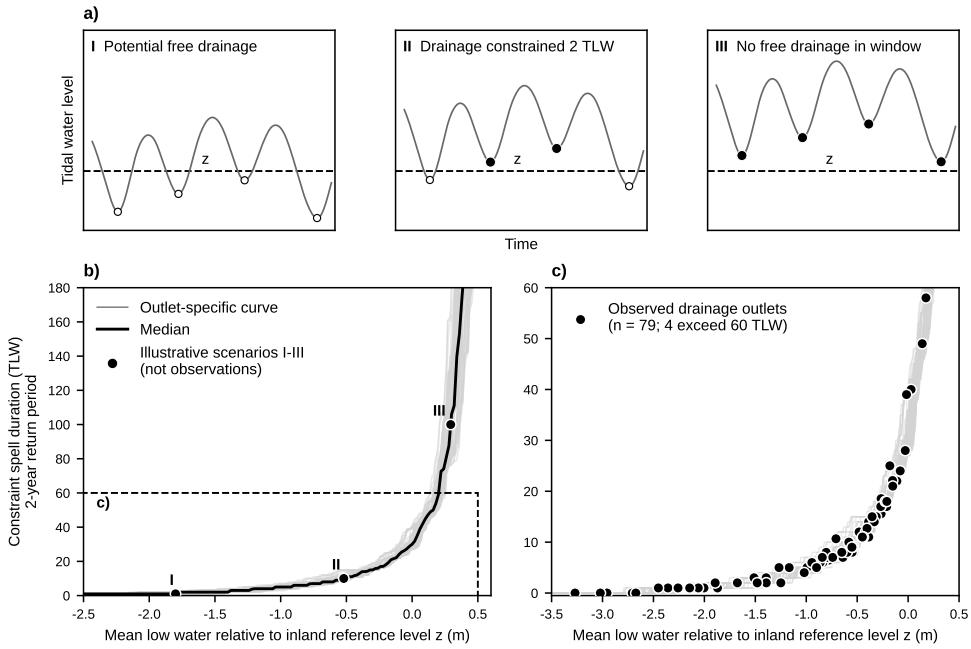


Fig. 2 Drainage constraint curves and present-day operating points. a) Conceptual representation of drainage constraints in a tidal environment. Free drainage is possible when coastal water levels fall below the outlet-specific inland reference level z (open circles), whereas drainage is constrained when the tidal low water (TLW) stays above z (filled circles). The three illustrative states represent potential free drainage (I), a constraint spell lasting two consecutive TLWs (II), and no free drainage opportunity within the displayed window (III); **b)** Outlet-specific 2-year return levels of constraint spell duration as a function of mean low water (MLW) relative to z. Grey lines show the outlet-specific constraint curves for 79 drainage outlets along the German North Sea coast. The black line shows their median. Points I–III correspond to the illustrative states in a) and represent a weakly constrained outlet (I), an outlet experiencing 2-year constraint spells with a flood-relevant duration of multiple days (II), and an outlet where drainage is constrained for a substantial part of the year (III); **c)** Zoomed-in view of b) with the 2-year constraint spell duration at the present-day operating point of each outlet, derived from the local MLW and the observed inland reference level. Black circles denote operating points; four outlets have return levels exceeding 60 TLWs and lie outside the displayed range. Grey lines show the individual outlet-specific constraint curves from b).

water level x (Figure 3). At one example outlet located on the lower, comparatively flat limb of its constraint curve, a 0.1 m increase lengthens the constraint duration by 3 consecutive TLWs (S_{local}= 3 TLW). At another example outlet, positioned on the steeper part of its curve, the same 0.1 m increase lengthens the constraint duration by 10 TLWs (S_{local}= 10 TLW) (Figure 3a).

Present-day sensitivities vary strongly among the 79 outlets, ranging from near-insensitive responses of $S_{local} \leq 1$ TLW per 0.1 m to increases exceeding 20 TLW per 0.1 m with a median of 1.5 TLW (interquartile range 0.5 to 3.0). This variation reflects both the outlet-specific shape of the constraint curve and the position of the operating point on that curve. Outlets situated on a low-gradient limb show limited changes

under an incremental relative water level increase, whereas outlets on the steep section show substantially larger increases in the 2-year constraint duration.

The spatial distribution of local sensitivity shows no clear regional pattern (Figure 3b). Instead, highly and weakly sensitive outlets occur across the study area, including within the same estuary or along nearby sections of coastline. Geographically proximate drainage outlets could therefore respond differently to an identical relative water level change. This small-scale heterogeneity indicates that sensitivity cannot be inferred from location alone, but depends on the interaction between outlet-specific inland reference levels (due to catchment characteristics) and coastal or estuarine water level dynamics.

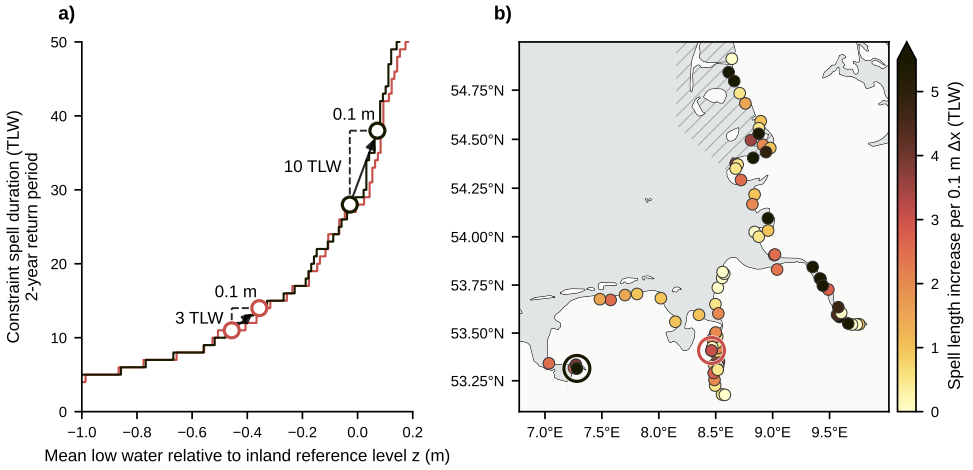


Fig. 3 Local sensitivity of drainage constraints to relative water level change. a) Construction of the local sensitivity to relative water level change, expressed as the constraint curve slope $\Delta RL2/\Delta x$ (S_{local}) for two example outlets. Step curves show the 2-year return level ($RL2$) of drainage constraint spell duration as a function of relative water level x, the difference between mean low water (MLW) and the inland reference level z. For one outlet (red) a rise of 0.1 m in relative water level lengthens the $RL2$ by 3 tidal low waters (TLWs); for the other outlet (black), located on a steeper section of its curve, the same rise increases the duration by 10 TLWs; **b)** S_{local} for all analysed outlets along the German North Sea coast, expressed as the increase in the $RL2$ per 0.1 m rise in relative water level. Dark markers denote highly sensitive outlets on the steep limb of their constraint curves and pale markers denote weakly sensitive outlets. The locations of the example outlets in a) are circled in black and red. S_{local} is reported as the median across a $\pm$ 0.30 m inland reference level band, and the hatched area indicates higher TLW uncertainty (see Methods). Colour scale is truncated at the 85$^{\text{th}}$ percentile.

Relative water level rise increases the probability of prolonged drainage constraints

Relative water level rise also increases the frequency of prolonged drainage constraints. Present-day constraint duration and sensitivity describe complementary aspects of

drainage-system state, but do not directly indicate how close an outlet is to a marked change in the frequency of prolonged constraints. This proximity is quantified by the relative water level change needed to transform a presently rare 20-year return period constraint duration into a 2-year return period event ($\Delta x_{20:2}$). The 20-year return period reflects the empirical frequency, supported by the length of the observed data series. Considering less frequent events would require return period extrapolation based on an assumed probability distribution. For each outlet, the present-day 20-year return period constraint duration was identified on the corresponding 20-year constraint curve. The same duration was then located on the 2-year curve, and the horizontal distance between the two positions was defined as $\Delta x_{20:2}$ (Figure 4a). A small $\Delta x_{20:2}$ value means that only a small relative water level increase is sufficient for the same constraint duration to shift from a 20-year to a 2-year event, whereas a large value means that a greater increase in relative level is required for the same frequency amplification.

Across the analysed outlets (Figure 4b), median $\Delta x_{20:2}$ is 0.32 m, with an interquartile range of 0.24 m to 0.50 m. At 18 % of outlets, a relative water level increase of less than 0.20 m would be enough for a constraint duration currently expected once in 20 years to recur approximately every two years. Other outlets require increases approaching or exceeding 0.50 m.

As with local sensitivity, $\Delta x_{20:2}$ values show high spatial heterogeneity. Low $\Delta x_{20:2}$ values occur both within estuaries and along the open coast, and neighbouring drainage outlets can differ considerably. Outlets with high local sensitivity generally exhibit lower $\Delta x_{20:2}$, indicating that a strong response to incremental relative water level change often coincides with a smaller shift required for frequency amplification.

Discussion

Our results show that drainage constraints in diked coastal lowlands are governed by a non-linear interaction between TLWs and inland reference levels. Across 79 drainage outlets, the duration of drainage constraints increases gradually while MLW remains multiple metres below the inland reference level, but rises rapidly as the two levels converge. The accelerating increase in constraint duration results from the progressive loss of free drainage. As MLW rises relative to the inland reference levels, low tides that previously interrupted constraint spells increasingly stay above the inland reference level, merging separate constraint spells into longer periods without free drainage. A comparable response has been reported for a managed LECZ catchment, where modelled hinterland flood duration increased only gradually under moderate SLR but sharply beyond a critical level, because elevated TLWs increasingly prevented free drainage [18]. Such threshold-like dynamics are consistent with non-linear responses in hydrological [31] and coastal systems [32, 33]. Although the outlet-specific curves exhibit a common qualitative form, present-day operating points and sensitivities vary substantially among outlets. These findings demonstrate that gradual changes in relative water level can produce disproportionate changes in both the duration and frequency of drainage constraints, but that the magnitude of this response is strongly site-specific. One implication is that, for around 20 % of the outlets, the relative water level increase

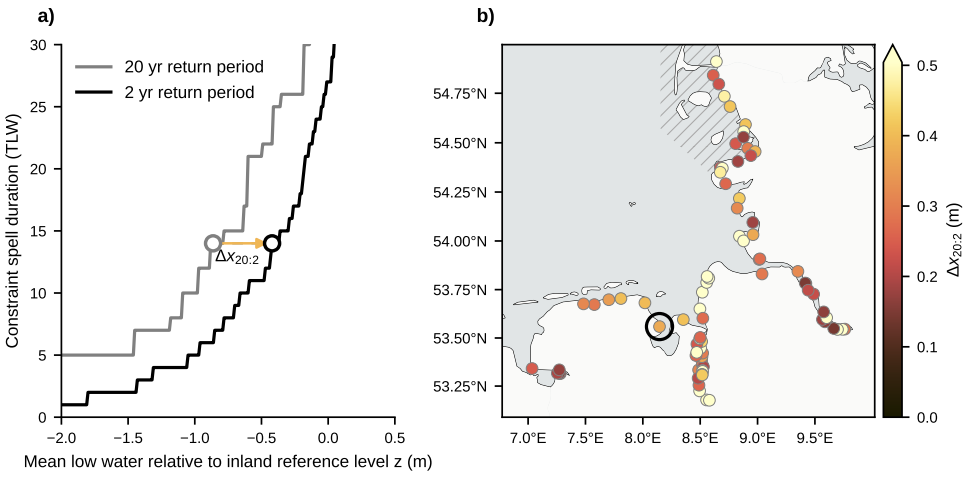


Fig. 4 Relative water level rise required for a present-day 20-year drainage constraint duration to become a 2-year event ($\Delta x_{20:2}$). a) Construction of the $\Delta x_{20:2}$ metric for an exemplary outlet. Step curves show the empirical 2-year (black) and 20-year (grey) return levels of drainage constraint duration as a function of mean low water (MLW) relative to the inland reference level. The present-day 20-year return level (open grey circle) is projected horizontally onto the 2-year curve (open black circle); the horizontal distance $\Delta x_{20:2}$ is the rise in relative water level at which this constraint duration becomes a 2-year event; **b)** Median $\Delta x_{20:2}$ required to amplify the frequency of a 20-year constraint duration to a 2-year event at each drainage outlet along the German North Sea coast. Darker markers indicate outlets where a smaller rise in relative water level is sufficient to amplify a present-day 20-year constraint duration to a 2-year event. The hatched area indicates higher tidal low water uncertainty (see Methods). Colour scale is truncated at the 75$^{\text{th}}$ percentile.

that converts a presently 20-year constraint duration into a 2-year event lies within the SLR range projected for the German Bight by 2050 (median across SSP1-2.6 to SSP5-8.5: 0.25 m to 0.29 m at Cuxhaven relative to 1995–2014) [34]. As more frequent prolonged constraints increase the likelihood that reduced drainage capacity co-occurs with other flood drivers, this frequency amplification increases inland flood hazard.

The event-based drainage constraint framework developed here extends conventional flood hazard assessments in LECZs, which often emphasize extreme water levels, peak discharges and temporally aggregated coastal conditions [5, 6, 22–26, 28]. Duration-based approaches in tidal environments have been applied to storm-surge barrier closures, for example by quantifying sequences of successive tidal high waters that exceed a flood threshold [35–37]. These approaches, however, focus on the high water phase of the tidal cycle and do not explicitly account for low water, despite its critical role in determining drainage capacity [14]. By expressing coastal water levels in terms of their effect on free drainage, drainage constraints directly link coastal boundary conditions to drainage capacity. Constraint spells identify periods during which free drainage is insufficient to lower inland water to its reference level, and their duration determines how long accumulating water must be retained within the hinterland or removed by pumping to maintain operational water levels.

The distinction between the magnitude and the duration of coastal water level events is directly relevant to the design and assessment of coastal drainage infrastructure. Storage basins, channel networks and pumping stations must collectively manage the water accumulated during periods when drainage is constrained [38, 39]. The required capacity of the infrastructure therefore depends not only on the maximum coastal water level or the magnitude of an inland discharge, but also on the duration and frequency of drainage constraints [14, 24]. A short extreme coastal water level event may have limited consequences if free drainage resumes during the following low tide, whereas a sequence of elevated low waters can constrain free drainage over several tidal cycles and allow otherwise moderate rainfall or river discharge to accumulate and result in hinterland flooding [24]. Comparable duration effects are known from storm-surge barrier operation, where the volume of accumulated inland water scales with closure duration [37]. Our results show that such multi-day drainage constraints already recur at many outlets and their duration can increase markedly with modest rises in relative water level (Figure 2c, Figure 3b). From a water management perspective, the constraint duration governs how long available storage is depleted, pumping demand persists, and operational flexibility is reduced [14]. Local drainage infrastructure and storage capacity must therefore be adapted to these prolonged drainage constraints and the urgency for adaptation varies among systems. This need for adaptation is consistent with reports that some water boards along the North Sea coast increasingly operate their drainage systems close to capacity [7].

Although elevated coastal water levels are widely recognized as an important boundary condition for drainage design [38, 40], they are rarely characterized explicitly in terms of constraint duration and frequency. The drainage constraint framework developed here provides this characterization. A constraint spell with a selected return period can be applied directly as a boundary condition in storage and drainage design and in event-based compound-flood analyses. Compound flood analyses typically pair drivers within fixed time lags or windows, and their results have been shown to be sensitive to this choice [7, 41, 42]. In lowlands that rely on free drainage, constraint spells offer a physically based alternative, as they span the period in which free drainage is insufficient and thus provide a natural frame for analysing multivariate or temporally compounding events [21]. Relative to this constraint duration, coincident rainfall, river discharge and groundwater contributions can be evaluated together with the resulting storage demand, pumping requirements and post-event recovery. This allows the consistent evaluation of the drainage capacity of existing systems as sea levels, tidal characteristics, land elevation or operational reference levels change, which is particularly important for long-standing infrastructure exposed to evolving coastal and hinterland flood drivers.

Furthermore, adaptation-pathway studies often treat pumped hinterland drainage as a technically feasible response while omitting or simplifying the sea-level-dependent costs of operation, maintenance and infrastructure replacement [43–45]. The drainage constraint framework can further help identify not only hydraulic tipping points, at which free drainage becomes inadequate, but also economic or institutional limits beyond which continued drainage of affected areas is no longer viable, and other options including retreat may become necessary [46].

The three indicators developed here describe complementary aspects of present-day drainage constraints and sensitivity to relative water level change. The baseline 2-year constraint duration, $RL2$, identifies outlets where prolonged drainage constraints already govern drainage operation. The local sensitivity, S_{local}, identifies outlets in which a small incremental change in relative water levels produces a large increase in constraint duration. The frequency amplification metric, $\Delta x_{20:2}$, identifies systems where a presently rare constraint duration is close to becoming recurrent. Considered together, the metrics show that present-day constraint duration and sensitivity to further relative water level change are closely linked: outlets with long 2-year constraint durations are generally also among the most sensitive to rising MLW relative to the inland reference level. The $\Delta x_{20:2}$ metric adds a complementary perspective by quantifying how much change is required for a constraint currently associated with a 20-year return period to recur every two years. This is conceptually similar to the frequency amplification factor used in extreme sea level research, which quantifies how SLR increases the frequency of extreme coastal water levels [47–49].

The spatial heterogeneity of these indicators shows that regional coastal conditions alone are insufficient for evaluating drainage constraints. Highly and weakly sensitive outlets occur throughout the study area, and geographically proximate outlets occupy different positions on their constraint curves. This variability arises because the drainage constraint at each outlet depends on both the coastal or estuarine water levels and the outlet-specific inland reference level. On the seaside, TLWs can differ substantially over short distances, as tides change in phase and amplitude and become distorted by shallow-water effects along coasts and estuaries and across the complex morphology of the Wadden Sea [50–52]. Surge-driven water levels also vary spatially, depending on coastline orientation, shelf and estuarine geometry, and nonlinear tide–surge interaction [53, 54]. Therefore, the timing, duration and asymmetry of low water periods can differ even between neighbouring outlets. On the landside, operational target levels depend on local water management, land use, drainage practice and hinterland elevation [39]. Neighbouring outlets can therefore experience strongly different drainage constraints within the same estuary or coastal section. Regional adaptation strategies that apply uniform assumptions across coastal segments may consequently overlook locally sensitive outlets or prioritize outlets that remain comparatively robust to relative water level change. As the framework does not account for existing storage, pumping capacity or operational practices, translating these indicators into adaptation priorities requires additional outlet-specific assessments.

The relative water level relationship used here integrates several processes that may alter future drainage constraints. SLR raises the coastal water levels, while changes in tidal propagation caused by channel deepening, morphodynamic processes or altered friction may influence low water levels independently of mean SLR [55–59]. Land subsidence [60] and changes in inland water level management alter the reference level from the landward side. Episodic storm surges can further elevate successive TLWs and influence the upper tail of the constraint-duration distribution. The framework does not attribute an observed or projected change to any one of these processes. Rather, it quantifies their combined consequences for the hydraulic relationship that controls free drainage. This integrated perspective makes the approach suitable for scenario

analysis, but process attribution requires further information on sea level, tidal, land elevation and management changes.

While this study focuses on the German North Sea coast, the underlying mechanisms are broadly applicable to managed coastal lowlands worldwide. Many LECZs rely on similar drainage methods, where the interaction between inland water levels and coastal boundary conditions controls drainage capacity [8, 10, 12, 14]. Worldwide, low water levels are changing not only with mean SLR but also through changes in the tidal component, which vary locally in sign and magnitude and can amplify or partly offset mean SLR [61, 62]. Since our results show that constraint durations rise sharply as TLWs approach the inland reference level, even gradual changes in MLW may have disproportionate impacts on inland flood hazard by prolonging drainage constraints. Extreme coastal water levels and hinterland rainfall are compounding drivers [5, 7, 25], whereas sustained elevations in TLWs reduce the drainage capacity and thus influence both the event-based hazard and the system's ability to recover from floods [14, 18]. TLWs should therefore be considered alongside extreme sea levels and precipitation when assessing hinterland flood hazard. The proposed framework supports such assessments with minimal data requirements and requires only a sufficiently long TLW record and an estimate of the inland reference level. This makes it transferable to regions where operational data or calibrated drainage models are unavailable. Its value in such settings lies not in replacing local hydraulic modelling, but in providing a consistent first-order assessment of present-day constraint durations, their sensitivity to relative water level change, and their proximity to substantial shifts in event frequency.

Future work should extend the framework by incorporating projected changes in tidal water levels, SLR, land subsidence and local hydrological conditions to assess how these processes jointly alter the duration and persistence of drainage constraints. Coupling constraint spells with dynamic inland processes, particularly precipitation and river discharge, would allow an explicit assessment of compound interactions between inland water accumulation and constrained drainage. Combined with local knowledge of pumping capacity, storage availability and water level management practices, the framework can then support site-specific adaptation planning and risk assessments.

Overall, our results demonstrate that effective assessment of flood hazard and adaptation in coastal lowlands requires a shift from static representations of drainage capacity towards a dynamic, process-based understanding of how drainage constraints emerge from interactions between inland and coastal water levels. By characterizing these interactions and their non-linear effects on drainage constraints, this study provides a foundation for assessments of drainage system capacity under present and changing conditions. The principal advance of the framework is therefore not the recognition that high coastal water levels restrict drainage, but the conversion of this well-known hydraulic mechanism into an event-based variable with an explicit duration, frequency and sensitivity to relative water level change.

Limitations

Several limitations should be considered when interpreting these results. On the seaside, TLWs at ungauged outlets were reconstructed by spatial interpolation. Although this approach performs well in the estuaries and along most of the open coast, its skill is reduced in the morphodynamically complex North Frisian Wadden Sea (see Methods). Estimates for outlets in this region therefore carry greater uncertainty in both spell detection and MLW. Observed TLW trends also differ in sign between the open coast and the estuaries, consistent with previous studies [56, 57]; we therefore detrend all series to a common reference epoch. We do not extrapolate these trends because the effects of morphodynamic change in the Wadden Sea [52] and of SLR on estuarine tidal dynamics [63] remain highly uncertain and are beyond the scope of this study. More generally, using historical return periods assumes that the statistical properties of the observed record remain representative of present conditions. Non-stationarity in mean sea level, tidal dynamics and climate forcing may alter these distributions.

On the landside, the ALS-derived reference levels are based on a measurement method not designed specifically for water surfaces and represent only a snapshot of inland water levels at the time of survey. We assume that no flood conditions occurred during the surveys and assign an uncertainty band of $\pm$ 0.30 m, which integrates i) ALS measurement error and ii) the uncertainty of the drainage system state during the time of survey. This uncertainty is propagated through all derived metrics. Knowledge of local operational target levels would substantially reduce uncertainty, but such data are generally not publicly accessible in Germany. The inland reference level is also a simplified representation of the hydraulic threshold and does not account for spatial water level gradients or temporally varying target levels within drainage catchments. We assume that free drainage can lower the inland water to the reference level whenever a TLW falls below that level. In practice, free drainage requires a minimum hydraulic head to overcome hydraulic losses. This threshold is site-specific, depending on the outlet structure and the characteristics of the drainage system [64], which were not available for inclusion in this analysis.

A drainage constraint, as defined here, indicates that TLWs do not fall below the inland reference level, but it does not imply inland flooding. Actual impacts additionally depend on precipitation and river discharge, antecedent storage, groundwater conditions, channel conveyance, pumping capacity and operational decisions. Measures such as adaptive drainage management, temporary storage and pumping may mitigate inland flood hazard even when free drainage is constrained. The indicators presented here should therefore be interpreted as measures of the externally imposed boundary condition for drainage systems, rather than as direct estimates of flood probability.

Methods

Study region

The study focuses on low-lying, diked coastal lowlands along the German North Sea coast, extending from the Dutch–German border in the west to the Danish border in the north (Figure 1b). This coastline is characterized by extensive marshlands, tidal flats and estuaries [56, 57, 65], where natural drainage is strongly modified by flood

protection and water management infrastructure. Large parts of the hinterland lie at or below mean sea level and are protected by dike systems that decouple inland water levels from the open sea [66]. As a result, surface water drainage is controlled by tidal gates, pumping stations and combined structures, which regulate discharge from inland channel networks to the sea or tidal estuaries depending on the tidal stage [7, 67].

Coastal water level data

Coastal water level records, comprising TLW times and levels, were provided by the German Federal Institute of Hydrology. Apparent outliers were removed from the time series upon visual inspection and stations exhibiting pervasive data quality issues, such as undocumented jumps, were excluded entirely from further analysis. In total, 69 of 71 tidal gauging stations were retained for subsequent interpolation across the study region (Extended Data Fig. 1).

Interpolation of tidal low water levels

We divided the study region into five subsystems: the Elbe, Weser, Jade, and Ems estuaries, and the open German Bight coast. This division follows the German Federal Waterways and Shipping Administration, which assigns each of its tide gauges to one of these subsystems. Within each subsystem, we selected the gauge with the longest continuous record as the temporal reference. Records across the gauge network ranged from less than 3 years to more than 123 years (mean 58.5 years). The reference series provided a common sequence of TLW events to which observations from the remaining gauges were aligned.

TLW events at all stations in each subsystem were matched to the respective reference series using a strictly monotonic one-to-one matching procedure (i.e., each event is matched at most once and in chronological order). To account for tidal propagation within each subsystem and avoid ambiguity between successive tidal cycles, the occurrence times of TLW events at each station were first adjusted by the estimated median time lag relative to the reference gauge. Following this temporal adjustment, events were then matched within a $\pm$ 3 h tolerance window, with the monotonicity constraint ensuring that no event was reused and that the chronological order of the tidal cycle was preserved. The temporal adjustment was applied only for event matching, while the original occurrence times and water levels were retained for subsequent analyses. Where no matching TLW event could be identified within the tolerance window, no data value was assigned for that event at the respective station.

To extend tidal information beyond the gauged network to drainage infrastructure locations, spatial interpolation was performed separately for the estuaries and the open German Bight coast to reflect their distinct hydrodynamic characteristics. The estuaries were treated as quasi-one-dimensional systems dominated by longitudinal tidal propagation and damping, with each gauge assigned a river-kilometre coordinate measured along the waterway as a physically meaningful spatial reference. For each target location, the nearest upstream and downstream gauges within a 25 km search window were identified. Both the TLW levels and timing were then linearly interpolated along the river-kilometre coordinate between the contributing gauges.

The open German Bight coast was treated as a two-dimensional amphidromic system where we interpolated TLW levels and times using inverse distance weighting (IDW). All gauges within a 50 km radius of an outlet were included, provided that at least two gauges were available. We assigned weights proportional to $1/d^2$, where d is the horizontal distance between the gauge and the outlet. The larger search radius reflects the broader spatial coherence scales of the open basin relative to estuarine channels. A sensitivity analysis on the search radius showed that radii below approximately 40 km left too few gauges for interpolation, whereas larger radii extended the temporal coverage of the reconstructed series at the cost of a slight loss in reconstruction quality. Differences in mean root mean square error (RMSE), bias and R^2 between the tested radii were small (Extended Data Tab. 1), and the 50 km radius was chosen as a trade-off between temporal coverage and reconstruction quality. We selected IDW for its transparency, minimal parametrization, and deterministic nature, which facilitates direct comparison between observed and reconstructed values without imposing strong structural assumptions.

Interpolation skill was assessed using a leave-one-out cross-validation, whereby each gauge was sequentially withheld, its tidal metrics reconstructed from contributing stations, and predictions compared to observations using the RMSE. The interpolation performed well across most locations; however, reduced skill was observed in the North Frisian Wadden Sea (Extended Data Fig. 1). In this region, performance was limited by the exceptional hydromorphodynamic complexity – including fragmented barrier islands, irregular multi-channel geometries, and extensive intertidal flats – which produces tidal patterns that are insufficiently resolved by the sparse local gauge network [52, 68, 69]. Results from this area should therefore be interpreted with caution. The validated interpolation schemes were subsequently applied to reconstruct the TLW time series from 69 tide gauges at drainage outlet locations across the subsystems.

Analysis window and detrending

The outlet-specific interpolated TLW data were trimmed to a fixed common time window spanning two nodal cycles, from 1985 to 2022. Outlets with less than 95 % of the expected number of TLWs ($\approx$ 705 per year) within the window were excluded, leaving 79 drainage outlets for analysis. We detrended each TLW series to remove long-term changes in the mean water level during the analysis period. For each outlet, we calculated annual mean TLW, estimated its linear trend using the Theil–Sen slope, and subtracted the resulting trend from the individual TLW values. Detrended levels were referenced to the end of the analysis period (Extended Data Fig. 2). Trend significance was assessed with the Mann–Kendall test ($\alpha = 0.05$), but all series were detrended irrespective of significance to avoid artificial discontinuities at the significance boundary. The detrended series were used to calculate the outlet-specific MLW used throughout the analysis.

Inland reference water levels

Large-scale assessments of drainage-related flood hazard in diked LECZs are constrained by limited access to operational target levels, which are site-specific and

often not publicly available. Satellite laser altimetry has been shown to provide physically meaningful water surface elevations for large rivers, lakes, and reservoirs from regional to global scales [70–72]. Other remote sensing data sources, such as the radar-interferometer-based Surface Water and Ocean Topography mission, are too coarse to resolve many of the small water bodies in our study area [73]. We therefore extract surface water levels from 1 m × 1 m resolution ALS-derived digital elevation models (DEMs) for the German federal states of Lower Saxony [74] and Schleswig-Holstein [75]. This resolution resolves narrow drainage channels and small water bodies near coastal drainage outlets. Although ALS surveys are repeated only intermittently and therefore cannot capture inland water level dynamics directly, water levels in managed coastal drainage systems are generally maintained near operational target levels. A single survey can therefore provide a representative estimate of the local operational target level. We use this estimate as the inland reference level z against which coastal water levels are evaluated.

We identified coastal drainage outlets along the German North Sea coast using publicly available datasets of drainage infrastructure [76, 77]. For each outlet, we manually selected a reference location on the inland water surface immediately upstream of the outlet, using satellite imagery to avoid areas affected by nearby structures or vegetation where possible. At each location, we extracted elevations from the 1 m × 1 m ALS dataset within a 3 m radius. As channel widths varied, the extracted area potentially included raster cells on the sloping channel banks as well as on the water surface. We therefore used the mean of the lowest 30 % of elevations at each location as a proxy for the inland water level to reduce the influence of the higher bank elevations. The vertical accuracy of the used DEMs is $\leq \pm$ 0.15 m in flat to gently sloping open terrain and $\leq \pm$ 0.30 m in steep or densely vegetated terrain [74, 75]. We evaluated the derived reference levels against known operational target levels of ten drainage systems in Lower Saxony and the mean water level (MW) at 21 coastal drainage outlets in Schleswig-Holstein [78] along the German North Sea coast. The derived inland levels agreed closely with these available observations of MW (RMSE = 0.26 m) and with operational target stages (RMSE = 0.27 m) (Extended Data Fig. 3). This agreement supports using ALS-derived elevations as proxies for operational target levels. Based on the validation errors and the reported accuracy of the elevation data, we assigned each observed inland reference level an uncertainty of $\pm$ 0.30 m and propagated this uncertainty through all derived metrics.

We excluded coastal segments where drainage processes could not be reliably characterized. These include undeveloped or weakly drained shorelines, major harbour areas and tidally influenced oxbow lakes, for which identifying the relevant drainage system would require detailed local information. The Kiel Canal and Ems-Jade Canal were excluded because their regulated, bidirectional flow regimes are not representative of typical hinterland drainage. Drainage systems upstream of storm-surge barriers were omitted because barrier operation substantially alters tidal propagation and observed water levels in the protected reaches. Using this approach, we derived inland reference water levels for 79 coastal drainage outlets.

Drainage constraint spell analysis

Sequences of elevated TLWs are particularly relevant for drainage operations because they constrain drainage capacity over several tidal cycles. We characterize such situations using an outlet-specific threshold-based spell analysis based on the identified inland reference level at each coastal drainage outlet.

Definition of constraint spells

At each drainage outlet, we defined the local inland reference water level as a threshold and compared it with the spatially interpolated TLW levels seaward of that outlet. Individual TLWs were classified as an exceedance when they remained above this threshold, indicating that free drainage could not lower inland water to the reference level during that tidal cycle. Consecutive exceedances were grouped into constraint spells. A spell starts and ends with an exceedance and is terminated only by at least two consecutive below-threshold low waters. A single below-threshold low water between exceedances is therefore bridged and counted for the constraint duration, because one potential DW is unlikely to provide sufficient relief when hinterland water levels are already elevated. The constraint duration is defined as the number of TLWs spanned, including bridged single non-exceedances. To avoid artificially extending spells across missing TLW records, we split the record whenever the interval between successive low waters exceeded 1.75 times the expected semi-diurnal tidal interval of 12.4 h (this threshold is always exceeded when a single low water is missing), and any ongoing spell ended at the time series segment boundary.

Frequency analysis of drainage constraints

For each outlet and reference level threshold, we constructed an annual maximum series of constraint spell durations by hydrological year (01 November – 31 October). Multi-year spells were assigned such that every hydrological year intersected by a spell received its full duration as a candidate annual maximum. This maintains a monotonic response of return levels to the threshold, and avoids artificial saturation at the number of TLWs within a single year. Empirical return levels were then derived from the ranked annual maxima using Weibull plotting positions, which provide estimates of exceedance probability without assuming an underlying parametric distribution [79]. For a return period T, we selected the smallest annual maximum whose plotting position reached the corresponding probability $1 - 1/T$. For each outlet, we calculated 2- and 20-year return levels of constraint duration across a dense range of hypothetical inland reference levels. The range extended $\pm$ 0.50 m beyond the full range of detrended TLW values and was sampled at 0.01 m intervals. To enable comparison among outlets, constraint curves were expressed as a function of the relative water level difference between MLW and the inland reference level (Figure 2). Hence, increasing values represent either rising MLW or a decreasing inland reference level. The operating point of each outlet is its position on the constraint curve at the ALS-derived reference level. As constraint durations are integers, the resulting constraint curves are step functions. The overall workflow is visualized in the Extended Data Fig. 4.

Outlet-specific sensitivity S_{local}

We quantified local drainage sensitivity from the response of the $RL2$ of constraint duration to relative changes between MLW and the inland reference level z. For each outlet, local sensitivity was defined as the constraint curve slope $\Delta RL2/\Delta x$ (S_{local}) at the ALS-derived reference level, estimated by a central difference across a $\pm$ 0.10 m window and expressed as the change in $RL2$ per 0.10 m increase in relative water level x (Eq. 1), with $x = \mathrm{MLW} - z$. To assess the influence of uncertainty in the reference level observation on local sensitivity, we repeated the analysis for 0.01 m intervals across a $\pm$ 0.30 m band and report the median S_{local} for each outlet (Figure 3b).

$$S_{local}(x_0) = \tfrac{1}{2} \left| \mathrm{RL2}(x_0 + 0.1) - \mathrm{RL2}(x_0 - 0.1) \right| \quad (1)$$

Frequency amplification of drainage constraint duration

We defined $\Delta x_{20:2}$ as the increase in relative water level required for a constraint duration that currently has a 20-year return period to attain a 2-year return period. These return periods also span the range used to classify light and severe storm surges in Germany, providing an established context for distinguishing rare from recurrent coastal extremes [80]. Using Weibull plotting positions, we first estimated the typical duration of a 20-year event at the observed reference level. We then identified the smallest increase in relative water level at which an event of that duration becomes a 2-year event. This increase is equivalent to the distance between the 20-year and 2-year constraint curves ($\Delta x_{20:2}$) (Figure 4a). Smaller $\Delta x_{20:2}$ values therefore indicate outlets where a smaller increase in relative water level is sufficient to change a present 20-year constraint duration into an event occurring approximately once every two years.

Uncertainty in $\Delta x_{20:2}$ was estimated jointly from sampling uncertainty of the annual maximum series and uncertainty in the inland reference level. Sampling uncertainty was represented by resampling hydrological years and recalculating the return periods for each of 500 bootstrap replicates. Uncertainty of the reference level observation was represented by shifting the observed level across a $\pm$ 0.30 m band at 0.01 m intervals, yielding 61 reference level values around the ALS-derived observation. The combined bootstrap and reference level ensemble was used to derive the median, 95 % confidence interval and interquartile range (IQR) of $\Delta x_{20:2}$ for each outlet. To distinguish the individual contribution of sampling and reference level uncertainty, we also calculated a bootstrap-only confidence interval with the reference level fixed at its ALS-derived estimate, comparing it with the combined interval (Extended Data Fig. 5).

Declarations

Funding

The study was supported by the German Federal Ministry of Research, Technology and Space (BMFTR) through the project METAscales (Grant No. 03F0955A), as well as the northern German states within the scope of the German Marine Research Alliance (DAM) mission mareXtreme. H.M. has received funding from the Lower Saxony Ministry of Science and Culture through SPRUNG for the collaborative project "Future Lab for Water Management" (Grant No. 11-76251-1873/2022 (ZN3994)). N.G. has received funding from the European Research Council (ERC) under the European Union's Horizon 2020 research and innovation programme (Grant agreement No. 101123732).

Ethics approval and consent to participate

Not applicable

Consent for publication

Not applicable

Materials availability

Not applicable

Data availability

Recent tide gauge data are available via Pegelonline, operated by the German Federal Waterways and Shipping Administration (https://www.pegelonline.wsv.de). The historical tide gauge data were provided by the German Federal Institute of Hydrology and are available from the institute upon request. The 1 m digital elevation models are openly available from the State Agency for Geoinformation and Land Survey of Lower Saxony (https://opengeodata.lgln.niedersachsen.de) and the State Agency for Surveying and Geoinformation of Schleswig-Holstein (DGM1; https://opendata.schleswig-holstein.de/dataset/digitales-gelandemodell-1-dgm1). The Copernicus GLO-30 digital elevation model is available from https://doi.org/10.5069/G9028PQB, and the Global LiDAR Lowland DTM from https://doi.org/10.17632/v5x4vpnzds.1. Regionalized sea level projections were obtained from the IPCC AR6 Sea Level Projections database (https://doi.org/10.26050/WDCC/AR6.IPCC-DDC_AR6_Sup_SLPr). The datasets generated in this study will be archived in a Zenodo repository by the time of publication.

Code availability

The code used for the analysis and to produce the figures will be archived in a Zenodo repository upon publication.

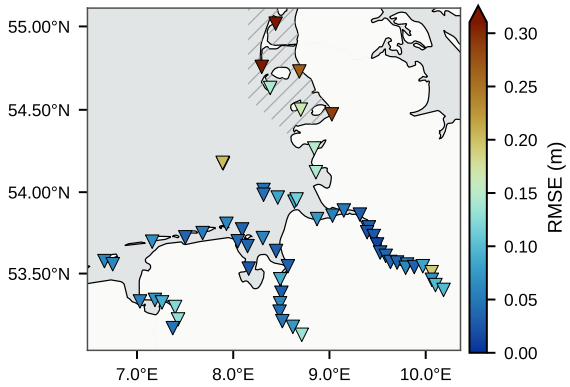
Author contributions

H.M. conceived the study, performed the analysis, created all visualizations, and wrote the original draft. C.J. interpolated the tidal water level data and contributed to the original draft. J.T. contributed to the processing of geospatial data. J.E., G.D. and N.G. reviewed and provided feedback for the manuscript. K.S. conceived the study, reviewed, and provided feedback for the manuscript.

Competing interests

The authors declare no competing interests.

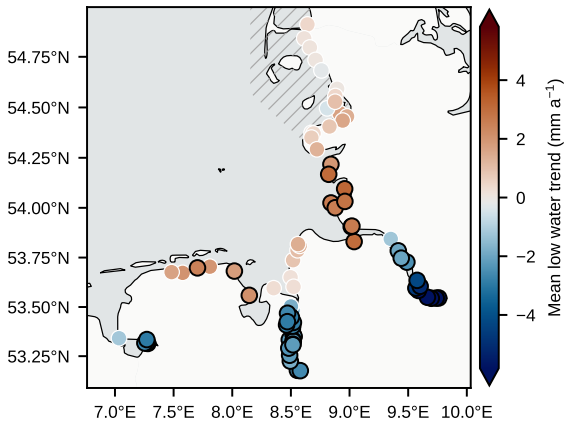
Extended Data



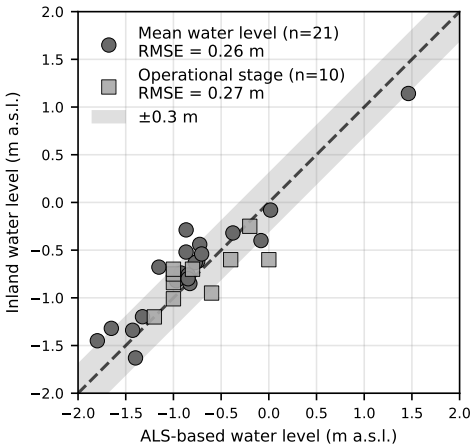
Extended Data Fig. 1 Leave-one-out cross-validation of interpolated tidal low water levels. Triangles indicate locations of tidal gauges and are coloured by the root mean square error (RMSE) of the interpolated tidal low water (TLW) level obtained by withholding that station and reconstructing its TLW series from the remaining gauges. RMSEs are below 0.05 m along most of the open coast and in the estuaries, but exceed 0.15 m at several stations in the North Frisian Wadden Sea. The hatched area marks the region in which TLW interpolation is considered less reliable (RMSE $>$ 0.15 m) as the interpolation in these areas proved difficult because the low water propagation between the islands and across intertidal flats is strongly modified by local bathymetry and drying. This increased uncertainty may affect the detection and characterization of drainage constraint spells in this region.

Extended Data Tab. 1 Sensitivity of the inverse distance weighting reconstruction of tidal low waters to the search radius. All values are means across the validation gauges; 40 km is the smallest radius for which sufficient gauges are available for interpolation; 50 km was used in this study.

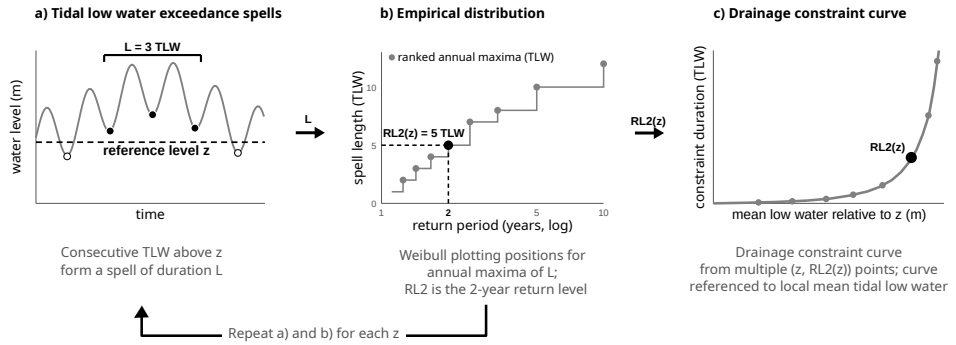
Radius (km)	RMSE (m)	Bias (m)	R^2	Coverage (years)
40	0.1339	0.0019	0.8752	51.9794
50	0.1340	0.0000	0.8709	54.5717
60	0.1378	0.0014	0.8591	56.2182



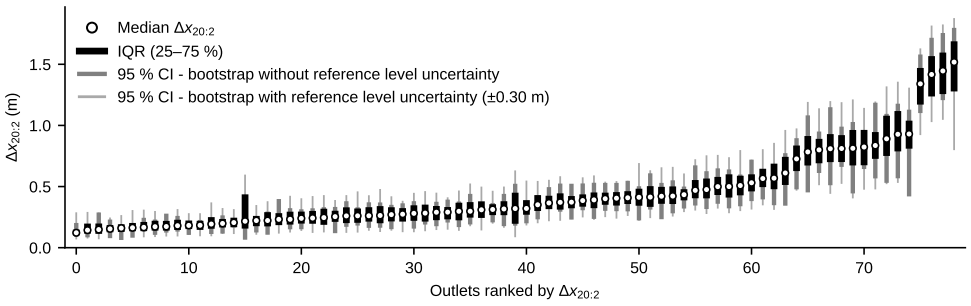
Extended Data Fig. 2 Spatial distribution of mean low water trends along the German North Sea coast. Colours show the Theil–Sen slope in annual mean tidal low waters at each drainage outlet in millimetres per year. Trends were estimated over a period of two nodal cycles, from 1985 to 2022. Markers outlined in black indicate statistically significant trends according to the Mann–Kendall test ($\alpha = 0.05$). The hatched region indicates higher uncertainty in the interpolation of tidal low water levels (see Methods for more details).



Extended Data Fig. 3 Validation of ALS-derived inland reference levels. Comparison of ALS-derived water-surface elevations with observed mean water levels at 21 coastal drainage outlets and operational target stages at ten drainage systems. The dashed line indicates a one-to-one relationship. The shaded band shows the assumed uncertainty of ± 0.30 m, accounting for elevation measurement error and variation in drainage-system conditions at the time of the ALS survey.



Extended Data Fig. 4 Workflow for deriving drainage constraint curves. a) At each outlet, detrended tidal low waters (TLWs) are compared with the inland reference level z. Consecutive exceedances form a spell of the duration L. Intervals exceeding 1.75 × 12.4 h are treated as data gaps and always break spells. **b)** Annual maxima of L per hydrological year are ranked using Weibull plotting positions. The 2-year return level $RL2(z)$ is the smallest annual maximum whose plotting position reaches a non-exceedance probability of 0.5, preserving the integer nature of spell durations. **c)** Repeating a) and b) across a dense grid of hypothetical reference levels (0.01 m steps) yields one (z, $RL2(z)$) pair per level. Curves are expressed relative to the outlet's detrended mean low water (MLW), so increasing values represent either rising MLW or a lower inland reference level.



Extended Data Fig. 5 Uncertainty decomposition of the $\Delta x_{20:2}$ metric. Drainage outlets ranked by median $\Delta x_{20:2}$ that converts the 20-year constraint duration into a 2-year event. For each outlet, the light grey interval shows the combined 95 % confidence interval from bootstrap resampling of observation years (n = 500) pooled with the ± 0.30 m inland reference-level uncertainty; the dark grey interval shows the bootstrap-only confidence interval with the reference level fixed at its observed value; the black interval shows the interquartile range of the combined ensemble.

References

[1] MacManus, K., Balk, D., Engin, H., McGranahan, G. & Inman, R. Estimating population and urban areas at risk of coastal hazards, 1990–2015: How data choices matter. *Earth System Science Data* **13**, 5747–5801 (2021).

[2] Magnan, A. K. *et al.* Sea level rise risks and societal adaptation benefits in low-lying coastal areas. *Scientific Reports* **12**, 10677 (2022).

[3] McGranahan, G., Balk, D. & Anderson, B. The rising tide: Assessing the risks of climate change and human settlements in low elevation coastal zones. *Environment and Urbanization* **19**, 17–37 (2007).

[4] Kulp, S. A. & Strauss, B. H. New elevation data triple estimates of global vulnerability to sea-level rise and coastal flooding. *Nature Communications* **10**, 4844 (2019).

[5] Bevacqua, E. *et al.* More meteorological events that drive compound coastal flooding are projected under climate change. *Communications Earth & Environment* **1**, 47 (2020).

[6] Ganguli, P. & Merz, B. Extreme Coastal Water Levels Exacerbate Fluvial Flood Hazards in Northwestern Europe. *Scientific Reports* **9**, 13165 (2019).

[7] Bormann, H., Kebschull, J., Gaslikova, L. & Weisse, R. Model-based assessment of climate change impact on inland flood risk at the German North Sea coast caused by compounding storm tide and precipitation events. *Natural Hazards and Earth System Sciences* **24**, 2559–2576 (2024).

[8] Schultz, E. From Natural to Reclaimed Land: Land and Water Management in the Polders of the Netherlands. *Water International* **8**, 55–60 (1983).

[9] Jenkins, K. *et al.* Exploring the Role of Strategic Place-Based Risk Assessment as a Framework to Support System-Based Climate Adaptation Planning. *Earth's Future* **14**, e2025EF007417 (2026).

[10] Adnan, M. S. G. *The Legacy of Polders: Diagnosing Complex Flooding Processes and Adaptation Options in the Coastal Region of Bangladesh.* Ph.D. thesis, University of Oxford, Oxford (2020).

[11] Liu, C. *et al.* Coastal development history and tidal flat ecosystem conservation along the coast of Jiangsu Province, China. *Journal of Coastal Conservation* **23**, 857–867 (2019).

[12] Rillahan, C. B., Alcott, D., Castro-Santos, T. & He, P. Activity Patterns of Anadromous Fish below a Tide Gate: Observations from High-Resolution Imaging Sonar. *Marine and Coastal Fisheries* **13**, 200–212 (2021).

[13] Titus, J. G. *et al.* Greenhouse Effect, Sea Level Rise, and Coastal Drainage Systems. *Journal of Water Resources Planning and Management* **113**, 216–227 (1987).

[14] Waddington, K., Khojasteh, D., Marshall, L., Rayner, D. & Glamore, W. Quantifying the Effects of Sea Level Rise on Estuarine Drainage Systems. *Water Resources Research* **58**, e2021WR031405 (2022).

[15] Federal Institute of Hydrology. ManMadeObject-DE. https://geoportal.bafg.de (2019).

[16] Santos, V. M. *et al.* Statistical modelling and climate variability of compound surge and precipitation events in a managed water system: A case study in the Netherlands. *Hydrology and Earth System Sciences* **25**, 3595–3615 (2021).

[17] Gold, A. C., Brown, C. M., Thompson, S. P. & Piehler, M. F. Inundation of Stormwater Infrastructure Is Common and Increases Risk of Flooding in Coastal Urban Areas Along the US Atlantic Coast. *Earth's Future* **10**, e2021EF002139 (2022).

[18] Walsh, S. & Miskewitz, R. Impact of sea level rise on tide gate function. *Journal of Environmental Science and Health, Part A* **48**, 453–463 (2013).

[19] Khojasteh, D., Glamore, W., Heimhuber, V. & Felder, S. Sea level rise impacts on estuarine dynamics: A review. *Science of The Total Environment* **780**, 146470 (2021).

[20] Bormann, H., Kebschull, J., Ahlhorn, F., Spiekermann, J. & Schaal, P. Modellbasierte Szenarioanalyse zur Anpassung des Entwässerungsmanagements im nordwestdeutschen Küstenraum. *Wasser und Abfall* **20**, 60–66 (2018).

[21] Zscheischler, J. *et al.* A typology of compound weather and climate events. *Nature Reviews Earth & Environment* **1**, 333–347 (2020).

[22] Moftakhari, H. R., Salvadori, G., AghaKouchak, A., Sanders, B. F. & Matthew, R. A. Compounding effects of sea level rise and fluvial flooding. *Proceedings of the National Academy of Sciences* **114**, 9785–9790 (2017).

[23] Gori, A., Lin, N. & Smith, J. Assessing Compound Flooding From Landfalling Tropical Cyclones on the North Carolina Coast. *Water Resources Research* **56**, e2019WR026788 (2020).

[24] van den Hurk, B., van Meijgaard, E., de Valk, P., van Heeringen, K.-J. & Gooijer, J. Analysis of a compounding surge and precipitation event in the Netherlands. *Environmental Research Letters* **10**, 035001 (2015).

[25] Wahl, T., Jain, S., Bender, J., Meyers, S. D. & Luther, M. E. Increasing risk of compound flooding from storm surge and rainfall for major US cities. *Nature Climate Change* **5**, 1093–1097 (2015).

[26] Heinrich, P. *et al.* Compound flood events: Analysing the joint occurrence of extreme river discharge events and storm surges in northern and central Europe. *Natural Hazards and Earth System Sciences* **23**, 1967–1985 (2023).

[27] Zscheischler, J. *et al.* Future climate risk from compound events. *Nature Climate Change* **8**, 469–477 (2018).

[28] Couasnon, A. *et al.* Measuring compound flood potential from river discharge and storm surge extremes at the global scale. *Natural Hazards and Earth System Sciences* **20**, 489–504 (2020).

[29] European Space Agency. Copernicus Global Digital Elevation Model. OpenTopography, https://doi.org/10.5069/G9028PQB (2021).

[30] Vernimmen, R. Global LiDAR Lowland DTM (GLL_DTM_v1). Mendeley Data, V1, https://doi.org/10.17632/v5x4vpnzds.1 (2020).

[31] Ross, C. A., Ali, G. A., Spence, C. & Courchesne, F. Evaluating the Ubiquity of Thresholds in Rainfall-Runoff Response Across Contrasting Environments. *Water Resources Research* **57**, e2020WR027498 (2021).

[32] Taherkhani, M. *et al.* Sea-level rise exponentially increases coastal flood frequency. *Scientific Reports* **10**, 6466 (2020).

[33] Sweet, W. V. & Park, J. From the extreme to the mean: Acceleration and tipping points of coastal inundation from sea level rise. *Earth's Future* **2**, 579–600 (2014).

[34] Garner, G. *et al.* IPCC AR6 WGI sea level projections. World Data Center for Climate at DKRZ, https://doi.org/10.26050/WDCC/AR6.IPCC-DDC_AR6_Sup_SLPr (2023).

[35] Chen, Z. & Orton, P. M. Effects of Storm Surge Barrier Closures on Estuary Saltwater Intrusion and Stratification. *Water Resources Research* **59**, e2022WR032317 (2023).

[36] Schönthaler, K. I-KH-4: Kettentiden. Tech. Rep., Bosch & Partner GmbH, Hamburg (2022).

[37] Chen, Z., Orton, P. & Wahl, T. Storm Surge Barrier Protection in an Era of Accelerating Sea-Level Rise: Quantifying Closure Frequency, Duration and Trapped River Flooding. *Journal of Marine Science and Engineering* **8**, 725 (2020).

[38] Normenausschuß Wasserwesen & Normenausschuß Maschinenbau. DIN 1184 - Part 1; Pumping stations; design, construction and operation (1992).

[39] Bormann, H. & Kebschull, J. Model based estimation of climate change impacts on the drainage demand of low lying coastal areas in Northwest Germany along the North Sea. *Journal of Hydrology: Regional Studies* **48**, 101451 (2023).

[40] Department for Environment, Food & Rural Affairs. National standards for sustainable drainage systems (SuDS) (2025).

[41] Hendry, A. *et al.* Assessing the characteristics and drivers of compound flooding events around the UK coast. *Hydrology and Earth System Sciences* **23**, 3117–3139 (2019).

[42] Xu, H. *et al.* Combining statistical and hydrodynamic models to assess compound flood hazards from rainfall and storm surge: A case study of Shanghai. *Hydrology and Earth System Sciences* **28**, 3919–3930 (2024).

[43] Völz, V. *et al.* The economically optimal mix and timing of coastal adaptation in Europe to 2150. *Nature Communications* **17**, 6249 (2026).

[44] Hall, J. W., Harvey, H. & Manning, L. J. Adaptation thresholds and pathways for tidal flood risk management in London. *Climate Risk Management* **24**, 42–58 (2019).

[45] Hinkel, J. *et al.* Coastal flood damage and adaptation costs under 21st century sea-level rise. *Proceedings of the National Academy of Sciences* **111**, 3292–3297 (2014).

[46] Haasnoot, M., Lawrence, J. & Magnan, A. K. Pathways to coastal retreat. *Science* **372**, 1287–1290 (2021).

[47] Hunter, J. A simple technique for estimating an allowance for uncertain sea-level rise. *Climatic Change* **113**, 239–252 (2012).

[48] Buchanan, M. K., Oppenheimer, M. & Kopp, R. E. Amplification of flood frequencies with local sea level rise and emerging flood regimes. *Environmental Research Letters* **12**, 064009 (2017).

[49] Vitousek, S. *et al.* Doubling of coastal flooding frequency within decades due to sea-level rise. *Scientific Reports* **7**, 1399 (2017).

[50] Friedrichs, C. T. & Aubrey, D. G. Non-linear tidal distortion in shallow well-mixed estuaries: A synthesis. *Estuarine, Coastal and Shelf Science* **27**, 521–545 (1988).

[51] Jänicke, L. *et al.* Assessment of Tidal Range Changes in the North Sea From 1958 to 2014. *Journal of Geophysical Research: Oceans* **126**, e2020JC016456 (2021).

[52] Jordan, C., Visscher, J. & Schlurmann, T. Projected Responses of Tidal Dynamics in the North Sea to Sea-Level Rise and Morphological Changes in the Wadden

Sea. *Frontiers in Marine Science* **8**, 685758 (2021).

[53] Horsburgh, K. J. & Wilson, C. Tide-surge interaction and its role in the distribution of surge residuals in the North Sea. *Journal of Geophysical Research: Oceans* **112**, 2006JC004033 (2007).

[54] Arns, A., Wahl, T., Dangendorf, S. & Jensen, J. The impact of sea level rise on storm surge water levels in the northern part of the German Bight. *Coastal Engineering* **96**, 118–131 (2015).

[55] Talke, S. A. & Jay, D. A. Changing Tides: The Role of Natural and Anthropogenic Factors. *Annual Review of Marine Science* **12**, 121–151 (2020).

[56] Kerner, M. Effects of deepening the Elbe Estuary on sediment regime and water quality. *Estuarine, Coastal and Shelf Science* **75**, 492–500 (2007).

[57] Hubert, K., Wurpts, A. & Berkenbrink, C. Interaction of Estuarine Morphology and adjacent Coastal Water Tidal Dynamics (ALADYN-C). *Die Küste* **89**, 25 (2021).

[58] Ebener, A., Jänicke, L., Arns, A. & Jensen, J. Untersuchungen zur Entwicklung der Tidedynamik an der deutschen Nordseeküste – Ein Ansatz zur Identifizierung und Quantifizierung von Tideveränderungen durch lokale Systemänderungen. *Die Küste* **89**, 30 (2021).

[59] Beemster, J. G. W. *et al.* Human footprint on estuarine tidal hydrodynamics. *Nature Geoscience* **19**, 620–629 (2026).

[60] Ohenhen, L. O. *et al.* Global subsidence of river deltas. *Nature* **649**, 894–901 (2026).

[61] Mawdsley, R. J., Haigh, I. D. & Wells, N. C. Global secular changes in different tidal high water, low water and range levels. *Earth's Future* **3**, 66–81 (2015).

[62] Haigh, I. D. *et al.* The Tides They Are A-Changin': A Comprehensive Review of Past and Future Nonastronomical Changes in Tides, Their Driving Mechanisms, and Future Implications. *Reviews of Geophysics* **58**, e2018RG000636 (2020).

[63] Khojasteh, D., Felder, S., Heimhuber, V. & Glamore, W. A global assessment of estuarine tidal response to sea level rise. *Science of The Total Environment* **894**, 165011 (2023).

[64] Bos, M. G. (ed.) *Discharge Measurement Structures* 3 edn. No. 20 in ILRI Publication (Internat. Inst. for Land Reclamation and Improvement, Wageningen, 1990).

[65] Benninghoff, M. & Winter, C. Recent morphologic evolution of the German Wadden Sea. *Scientific Reports* **9**, 9293 (2019).

[66] van den Hurk, B. *et al.* Living with sea-level rise in North-West Europe: Science-policy challenges across scales. *Climate Risk Management* **35**, 100403 (2022).

[67] Ahlhorn, F. *Hydrology of (Shallow) Coastal Regions*, 49–62. Wasser: Ökologie Und Bewirtschaftung (Springer Fachmedien Wiesbaden, Wiesbaden, 2018).

[68] Jacob, B. & Stanev, E. V. Understanding the Impact of Bathymetric Changes in the German Bight on Coastal Hydrodynamics: One Step Toward Realistic Morphodynamic Modeling. *Frontiers in Marine Science* **8**, 640214 (2021).

[69] Hagen, R., Winter, C. & Kösters, F. Changes in tidal asymmetry in the German Wadden Sea. *Ocean Dynamics* **72**, 325–340 (2022).

[70] Li, H., Zhang, J., Cai, X., Huang, H. & Wang, L. On the capacity of ICESat-2 laser altimetry for river level retrieval: An investigation in the Ohio River basin. *Journal of Hydrology* **626**, 130277 (2023).

[71] Zhang, G., Chen, W. & Xie, H. Tibetan Plateau's Lake Level and Volume Changes From NASA's ICESat/ICESat-2 and Landsat Missions. *Geophysical Research Letters* **46**, 13107–13118 (2019).

[72] Luo, S. *et al.* Satellite Laser Altimetry Reveals a Net Water Mass Gain in Global Lakes With Spatial Heterogeneity in the Early 21st Century. *Geophysical Research Letters* **49** (2022).

[73] Xu, H. *et al.* SDNet: A multi-scale SWOT framework for denoising and quality-control optimization in inland water body extraction. *GIScience & Remote Sensing* **63**, 2636315 (2026).

[74] State Agency for Geoinformation and Land Survey of Lower Saxony. Digitales Geländemodell - DGM1 - Niedersachsen. OpenGeoData.NI, https://opengeodata.lgln.niedersachsen.de (2024).

[75] State Agency for Surveying and Geoinformation of Schleswig-Holstein. Digitales Geländemodell 1. https://opendata.schleswig-holstein.de/dataset/digitales-gelandemodell-1-dgm1 (2025).

[76] Lower Saxony Ministry for Environment, Energy and Climate Protection. Umweltkarten Niedersachsen. https://www.umweltkarten-niedersachsen.de (2024).

[77] Schleswig-Holstein State Office for the Environment. Amtliches Wasserwirtschaftliches Gewässerverzeichnis. https://danord.gdi-sh.de/viewer/resources/apps/Wasserland_AWGV. Accessed 2025-12-09.

[78] Ministry for Energy Transition, Climate Protection, Environment and Nature of Schleswig-Holstein. Hochwasser-Sturmflut-Information Schleswig-Holstein. https:

//hsi-sh.de/pegelmap.html.

[79] Stedinger, J. R., Foufoula-Georgiou, E. & Vogel, R. M. in *Frequency analysis of extreme events* (ed.Maidment, D. R.) *Handbook of Hydrology* Ch. 18, 18.1–18.66 (McGraw-Hill, New York, 1993).

[80] Normenausschuß Wasserwesen. DIN 4049-3 Hydrology — Part 3; Terms for the quantitative hydrology (1994).